European Food Research and Technology (2020) 246:733–743
https://doi.org/10.1007/s00217-020-03442-x

ORIGINAL PAPER

New insights into the chemical bases of wine color evolution and stability: the key role of acetaldehyde

Martino Forino[1] · Luigi Picariello[1] · Annalisa Lopatriello[2] · Luigi Moio[1] · Angelita Gambuti[1]

Received: 7 November 2019 / Accepted: 18 January 2020 / Published online: 27 January 2020

Abstract

The reactivity of malvidin-3-*O*-glucoside with acetaldehyde, pyruvic and *p*-coumaric acids, was separately studied in wine model solution in the presence and absence of catechin, by UV–Visible spectrophotometry, NMR and Mass spectrometry. These naturally occurring metabolites were selected on account of their role in determining the red wine color. The scientific bases underlying the wine color are far from being fully clarified. Nonetheless, understanding the factors that govern the wine color is a crucial prerequisite for winemakers to implement appropriate technological practices to produce naturally stable high-quality wines. Among the investigated wine metabolites, acetaldehyde turned out to be the most reactive towards malvidin-3-*O*-glucoside by forming, as major products, ethylene-linked polymeric pigments that affected chromatic properties of the wine-like model solutions. Pyruvic acid and *p*-coumaric acid did not react with malvidin-3-*O*-glucoside, but in combination with catechin, they both determined a significant hypsochromic effect. Unexpectedly, in our model solutions, the formation of pyranoanthocyanins was not observed.

Keywords Red wine color · Acetaldehyde · Ethylene-linked pigment · Co-pigmentation · Malvidin-3-*O*-glucoside · NMR

Introduction

Wines are dynamic systems continuously changing in terms of chemical composition and sensory properties [1, 2]. The chemical transformations undergone by wines, especially during their maturation and aging periods, are mainly the results of redox reactions that often produce significant changes of both color and aroma. It follows that color intensity and stability are primary traits of high-quality and long-lasting red wines. The color of red wines is a complex phenomenon determined by many variables, among which pigments and co-pigmentation are major contributors [3]. Pigments are chemically correlated to phenolic compounds and particularly to anthocyanins, whose typical vivid red tints associated to their flavylium cations tend to disappear, as at typical wine pH levels, they quickly equilibrate with their colorless pseudobases [4] (Fig. 1a). Hence, any chemical transformations disrupting the anthocyanin π electron conjugation cause significant color changes in wines. It has been demonstrated that, beyond 5 years from bottling, most monomeric anthocyanins are found in wines only at low concentrations [5]. On the other hand, anthocyanins constitute a primary source of more structurally elaborated wine pigments that stabilize the wine color, since they are less prone to either degradation or bleaching; furthermore, their absorbance is stronger than that of monomeric anthocyanins and less influenced by pH variations [3]. Among the relatively wide selection of anthocyanin-derived pigments detected in wines, the family of pyranoanthocyanins is of primary importance. These compounds are formed by the reactions between anthocyanins and metabolites either produced during wine oxidation and fermentation, such as pyruvic acid and acetaldehyde, or extracted from grapes, such as cinnamic acids. When malvidin-3-*O*-glucoside (Mv3gl) reacts with pyruvic acid and acetaldehyde, vitisin-A (**1**) [6] and vitisin-B (**2**) [7] are, respectively, formed; the products of the reaction between anthocyanins and cinnamic acids are

Electronic supplementary material The online version of this article (https://doi.org/10.1007/s00217-020-03442-x) contains supplementary material, which is available to authorized users.

✉ Martino Forino
forino@unina.it

[1] Department of Agricultural Sciences, University of Napoli "Federico II"-Enology Sciences Section, Viale Italia, 83100 Avellino, Italy

[2] Department of Pharmacy, University of Napoli "Federico II", Via D. Montesano, 49, 80131 Naples, Italy

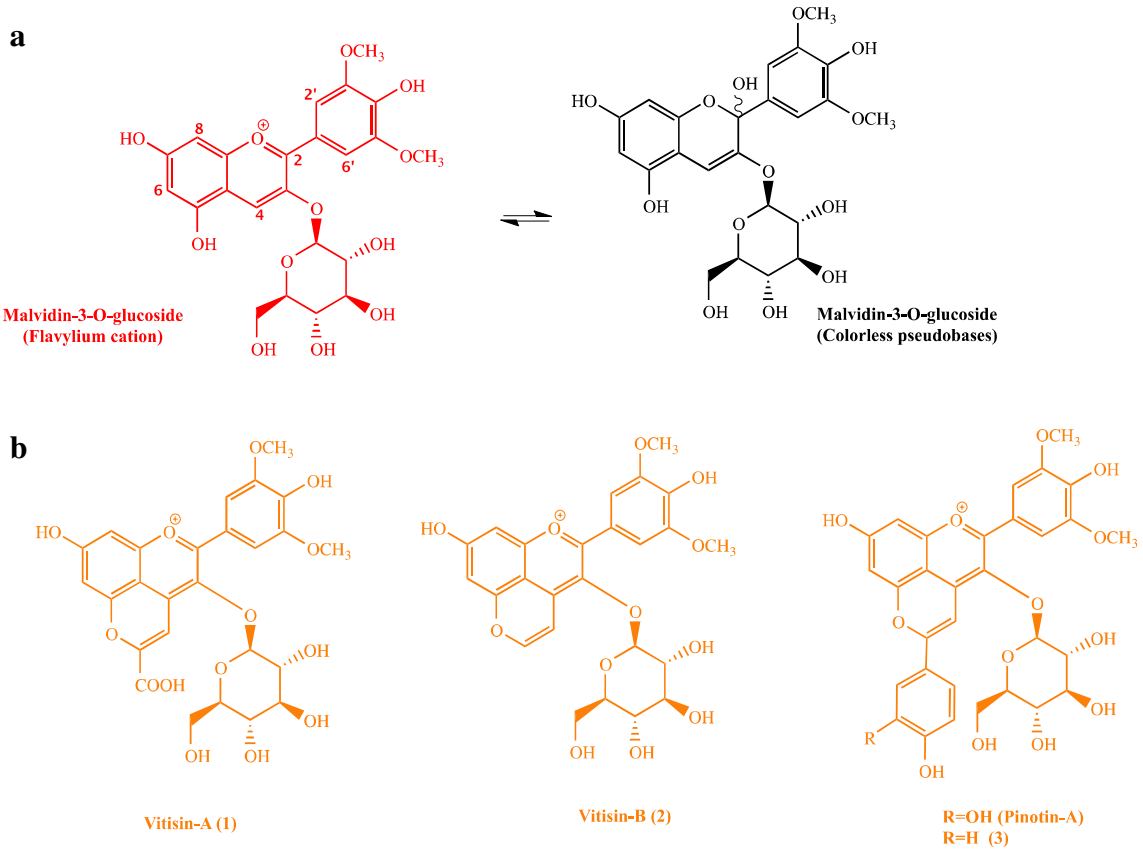

Fig. 1 **a** Mv3gl speciation: at typical wine pH range the red flavylium ion (left) quickly equilibrates with its colorless pseudobases (right). **b** chemical structures of the major wine pigments formed by the reaction of Mv3gl with pyruvic acid (vitisin-A, **1**) acetaldehyde (vitisin-B, **2**), and *p*-coumaric acid

generally referred to as pinotins [8] (Fig. 1b). Vitisin-A has been proven to resist to bleaching up to 250 mg/L of SO_2 in wine; vitisin-B is half bleached at 200 mg/L of sulfur dioxide; and both vitisin-A and -B are much more protected against bleaching than Mv3gl itself that is 80% bleached at a SO_2 concentration in wine as low as 50 mg/L [9]. Other important compounds contributing to the purple coloration of young wines are the ethylene-linked pigments produced by the reaction between acetaldehyde, Mv3gl and either catechin or epicatechin [10]. Such pigments are naturally formed during fermentation in the presence of acetaldehyde metabolically produced by yeasts [10].

As mentioned, another important factor determining the color of red wines is co-pigmentation, a weak association between anthocyanins and co-factors including flavonoids and phenolic acids. Co-pigments are usually responsible for hyperchromic shifts, resulting in higher absorbance values, and for both bathochromic and hypsochromic shifts in the wavelength of the observed absorbance maximum. The hypsochromic shift, generally in the 5–20 nm range, provides otherwise red solutions with blue–purple tints [3]. It is evident that the color of wines at the time of consumption is the result of many multifaceted and entwined factors including the specific grape metabolite composition and a series of production practices from the vineyard to the storage in the bottle and the study of red wine color is rather complicated. The understanding of the chemical behavior of wine colored compounds and how they evolve over time is a critical issue for winemakers to implement appropriate technological practices. Ultimately, the knowledge of the chemistry of wine color could suggest how to opportunely modulate the natural chemical composition of wine metabolites as to guarantee stable high-quality products.

Even though the chemistry of some of the reactants involved in the wine color has been investigated, a comprehensive and systematic study of their interactions and cross-reactivities has not been conducted yet. To advance the knowledge on the chemical bases of the wine color formation and evolution, we set up an experimental design based on a combination of UV–Visible spectrophotometry, NMR spectroscopy and high-resolution MS (HR-MS) spectrometry techniques to investigate the chemical behavior of Mv3gl in the presence of key wine metabolites including acetaldehyde, pyruvic acid, *p*-coumaric acid, and catechin.

Materials and methods

Chemicals and reagents

Malvidin-3-*O*-glucoside chloride (> 90% HPLC), pyruvic acid (98% HPLC), *p*-coumaric acid (98% HPLC), (+)-catechin (99% HPLC), pyruvic acid (99% HPLC), anhydrous acetaldehyde (99.5% GC), and tartaric acid (99% HPLC) were purchased from Sigma-Aldrich (Milan, Italy). Deuterated solvents were purchased from Cambridge Isotope Laboratories, Inc., (Tewksbury, MA, USA). Aqueous solutions were prepared with Milli-Q water from Millipore (Bedford, MA, USA).

Reaction solutions

All reaction solutions, arbitrarily termed in alphabetical order from A to F, were prepared in a tartrate buffer containing 5.0 g/L tartaric acid and brought to the pH level of 1.90. All the reaction solutions contained a calculated concentration of 2.5 mM for malvidin-3-*O*-glucoside; B, D and F solutions were also added with a calculated concentration of 2.5 mM for (+)-catechin. Acetaldehyde was added to the solutions A and B using a microdispenser to give a final concentration of approximately 3 mM. Solutions C and D contained 2.5 mM pyruvic acid; E and F contained 0.98 mM *p*-coumaric acid. The final volume of each reaction solution was 1.7 mL. All the reaction solutions contained in reaction flasks have been hermetically stored at 20 °C. Two replicates of the experiment were performed.

NMR and MS analyses

NMR experiments were run on a Varian Unity Inova 700 spectrometer equipped with a 13C Enhanced HCN Cold Probe and using a Shigemi 5 mm NMR tubes. A mixture of CD_3OD (δ_H 3.31; δ_C 49.0)/DCl (9:1) was used as deuterated solvent. ^{1}H-NMR, HSQC and HMBC standard Varian pulse sequences were employed. One-bond ^{1}H–^{13}C connectivities were determined by gradient 2D HSQC experiments, while two- and three-bond ^{1}H–^{13}C connectivities were determined by gradient 2D HMBC experiments optimized for a 2.3 J of 8 Hz. The time domain data matrix for the 2D NMR spectra was set at 4096 (F2) by 512 (F1) with 48 transients obtained per increment. Spectra were processed by zero-filling and Fourier transform to 4 K by 1 K data points after employing a sine filter multiplication. After 7 days of hermetical storage, from each reaction solutions (A-F) 700 µL were withdrawn, dried and finally solubilized in the deuterated solvent mixture.

HR-ESIMS and HR-ESIMS/MS in the positive ion mode experiments were carried out on a linear ion trap LTQ Orbitrap XL hybrid Fourier transform MS (FTMS) instrument equipped with an ESI ION MAX source (Thermo-Fisher). The following source settings were used for both HR-MS and HR collision-induced dissociation (CID) MS/MS: spray voltage 4,5 kV, capillary temperature 350 °C, capillary voltage 0 V, sheath gas 20 and auxiliary gas 21 (arbitrary units), and tube lens voltage 60 V, and 25% collision energy. Samples of each reaction solution were dried, solubilized in methanol and analyzed by continuous flow injection.

HPLC–DAD analyses

Solvents of HPLC-gradient grade and all other chemicals of analytical reagent grade were purchased from Sigma (Milan, Italy). The solutions were prepared in deionized water produced by a Purelab Classic system (Elga Labwater, Marlow, UK). Malvidin-3-*O*-glucoside chloride standard was used for calibration curves.

Analyses were performed according to the OIV Compendium of International Methods of Analysis of Wine and Musts (2017) in a HPLC Shimadzu LC10 ADVP apparatus (Shimadzu Italy, Milan), consisting of a SCL-10AVP system controller, two LC-10ADVP pumps, a SPD-M 10 AVP detector, and an injection system full Rheodyne model 7725 (Rheodyne, Cotati, CA) equipped with a 50 µL loop. A Waters Spherisorb column (250 × 4.6 mm, 4 µm particles diameter) with pre-column was used. Twenty µL of wine or calibration standards were injected into the column. Detection was performed by monitoring the absorbance signals at 518 nm, 280 nm and 360 nm. All the samples were filtered through 0.45 mm, Durapore membrane filters (Sigma-Aldrich, Milan, Italy) into glass vials and immediately injected into the HPLC system. The HPLC solvents were solvent A: water/formic acid/acetonitrile (87:10:3) v/v; solvent B: water/formic acid/acetonitrile (40:10:50) v/v. The gradient used was zero-time conditions 94% A and 6% B, after 15 min the pumps were adjusted to 70% A and 30% B, at 30 min to 50% A and 50% B, at 35 min to 40% A and 60% B, at 41 min, end of analysis, to 94% A and 6% B. After 10-min equilibrium period, the next sample was injected. The flow rate was 0.80 mL/min. For calibration, the external standard method was used: the calibration curve was plotted for the malvidin-3-*O*-glucoside (Extrasynthese, Lyon, France) on the basis of peak area and the concentration was expressed as mg/L of malvidin-3-*O*-glucoside. Two analytical replicates were carried out for each experimental replicate.

The same chromatographic conditions were used to separate the compounds formed in the reaction solutions A. A semi-preparative Luna 10u Column with a flow rate of 1.8 mL/min was employed and two peaks along with a

polymeric fraction were collected. The first peak was collected after 24 min; the second peak was collected after 30 min; the polymeric fraction was collected after 35 min and was not detected as a resolved peak.

Spectral measurements and CIELab parameter determination

A Shimadzu UV-1800 (Kyoto, Japan) UV spectrophotometer was used; 10 mm plastic cuvettes were used. Spectra were recorded between 400 and 800 nm. The CIELab coordinates, lightness (L^*), chroma (C^*), hue angle (Hue), red-greenness (a^*) and yellow-blueness (b^*) were determined according to CIE76 formula and the data were processed with the PANORAMA® software (LabCognition, Analytical Software GmbH & Co.KG for SHIDMAZU Deutschland GmbH, Duisburg). Color differences were also calculated as described by Gonzalez-Manzano et al. [11]. Two analytical replicates were carried out for each experimental replicate.

Results and discussion

The chemistry of Mv3gl is quite complex. Among other important chemical properties, the flavylium ion species of Mv3gl (**1**) possesses an electrophilic center at position 4 that can be attacked by natural nucleophiles occurring in musts and wines such as acetaldehyde, pyruvic acid and *p*-coumaric acid, to form the pyranoanthocyanins vitisin-B, vitisin-A and phenyl-pyranomalvidin-3-glucoside, respectively (Fig. 1b). Compound **1** is the most abundant species of Mv3gl at pH < 3, while as the pH increases, it readily equilibrates with its pseudobases, whose C4 is no longer an electrophilic center (Fig. 1a) [12]. It has been shown that already around a pH level of 3.3, the flavylium ion concentration appears reduced to almost ¼ that of its conjugate pseudobases [13]. Given that the formation of pyranoanthocyanins requires that C4 of Mv3gl be electrophilic, the pH level of our model solutions was adjusted to 1.9 to have the flavylium ion of Mv3gl as the predominant species in solution. Also, since the reported mechanism of the pyranoanthocyanin formation is subjected to an oxidation step following the addition of the nucleophile at the anthocyanin C4, we separately studied the Mv3gl reactivity with acetaldehyde, pyruvic acid and *p*-coumaric acid in the absence and in the presence of catechin. Catechin was instrumental to pursue a double purpose: first, its *ortho*-diphenol moiety has been proven to be crucially involved along with the atmospheric oxygen in the oxidation processes of wine [14] and, second, the simultaneous presence of catechin and Mv3gl in the reaction solutions was expected to shed some light on the possible competition between flavanols and anthocyanins in terms of reactivity towards the selected carbonyl compounds. In conclusion, our experimental design included three different pairs of reaction solutions as detailed below:

- Solution A: Mv3gl and acetaldehyde;
- Solution B: Mv3gl, acetaldehyde and catechin;
- Solution C: Mv3gl and pyruvic acid;
- Solution D: Mv3gl, pyruvic acid and catechin;
- Solution E: Mv3gl and *p*-coumaric acid;
- Solution F: Mv3gl, *p*-coumaric acid and catechin.

The molar ratio of each analyte was approximately 1:1, with the exception of *p*-coumaric acid and acetaldehyde. For the former, it was not possible to obtain a 1:1 ratio with either Mv3gl or catechin because of its reduced solubility in the wine model solution. In regards to acetaldehyde, given its volatility and difficulty in handling, it was added in slight excess to both solutions A and B.

All the above reaction solutions were analyzed by HPLC–DAD first after 2 h of storage at 20 °C for gaining preliminary information on the reaction progresses and again after 7 days, when a 700 µL aliquot was withdrawn from each reaction solution to be subjected to NMR- and HR-ESIMS-based analyses. Finally, by UV–Visible spectrophotometry, the colorimetric differences among the reaction solutions were determined.

Analysis of the reaction solutions containing Mv3gl, acetaldehyde (Solution A) and catechin (Solution B)

After 1 week of storage, by means of HPLC at the semi-preparative scale, from the reaction solution A, we isolated two peaks along with a polymeric fraction (SI.1). The ^{1}H-NMR analysis of the first peak led us to identify unreacted Mv3gl in its flavylium ion species by comparison of its spectroscopic data with those of an authentic sample (SI.2). The identity of the Mv3gl flavylium ion was further confirmed by a HR-ESIMS ion peak at *m/z* 493.1346 ($[C_{23}H_{25}O_{12}]^+$; $\Delta = 1.171$ ppm). Interestingly, along with the peak at 493, another quite intense ion peak was detected at *m/z* 547.1424 ($[C_{24}H_{28}O_{13}Na]^+$; $\Delta = 0.252$ ppm), implying 11 degrees of unsaturations (RDB = 10.5) (Fig. 2).To gain more insights into the chemical structure of this molecule, the ion peak at *m/z* 547 was subjected to HRMS-MS fragmentation. The first detected fragment, resulting from the loss of a neutral compound associated with a molecular formula of CH_4O, likely a methanol molecule, was centered at *m/z* 515.1151 ($[C_{23}H_{24}O_{12}Na]^+$; Δ =—1.722 ppm; RDB = 11.5). A second fragment ion peak at *m/z* 353.0628 ($[C_{17}H_{14}O_7Na]^+$; Δ =—1.031 ppm; RDB = 10.5) was reasonably generated by the loss of a glucosyl residue (Fig. 2). Such experimental evidence suggested that the molecule under investigation was a further species of Mv3gl deriving from the nucleophilic attack of a methanol molecule at the anthocyanin C2

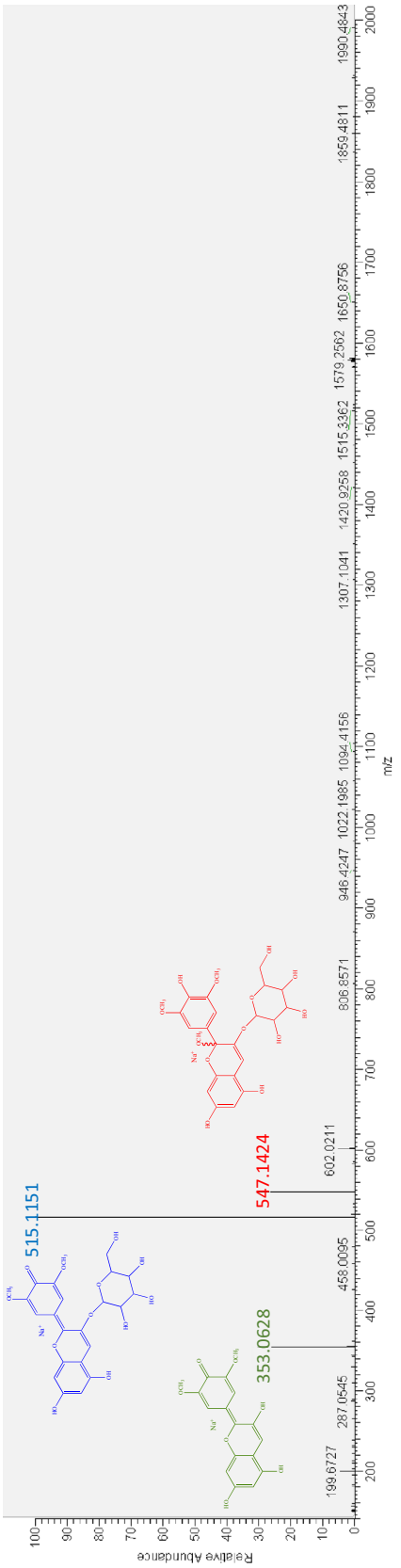

Fig. 2 HR-ESIMS–MS spectrum in the positive ion mode of the ion peak at *m/z* 547

position (Fig. 2). This compound may be an artifact considering that the analyzed fraction had been solubilized in pure methanol before being injected into the mass spectrometer. However, it is noteworthy that in addition to a water molecule, also a nucleophile as small as methanol is able to react with the electrophilic position 2 of the flavylium ion. To the best of our knowledge, it has never been reported that, besides water, other wine nucleophiles, including ethanol and sulfur dioxide, can react with such position. This provides an interesting datum about the optimal size of nucleophiles capable of reacting with the electrophilic C2 of the flavylium ion.

The second fraction obtained from the HPLC-based separation of the reaction solution A contained a methyl methine-linked Mv3gl dimer identified as **4** on account of its NMR data (SI.2; Fig. 3) superimposable with those reported by Atanasova et al. [15]. The HR-ESIMS confirmed our structural hypothesis. Accordingly, we detected ion peaks at *m/z* 1011.2785 ($[C_{48}H_{51}O_{24}]^+$; $\Delta = 2.038$ ppm), at *m/z* 1029.2866 ($[C_{48}H_{53}O_{25}]^+$; $\Delta = -0.411$ ppm), and at *m/z* 506.1422 ($[C_{48}H_{52}O_{24}]^{2+}$; $\Delta = 0.617$ ppm). These mass values were assigned to different forms of **4** as reported in Fig. 3. However, the most intense ion peak of the spectrum was centered at *m/z* 1043.3055 ($[C_{49}H_{55}O_{25}]^+$; $\Delta = 2.709$ ppm; RDB = 22.5). Subjected to MS–MS fragmentation, by losing a CH_4O neutral moiety, the peak at 1043 generated a fragment ion at 1011 assigned to a form of compound **4** as already discussed. Hence, similar to what we had already observed with the monomeric Mv3gl, we hypothesized that one Mv3gl subunit of **4** had reacted with a methanol molecule at position 2 (Fig. 3).

Finally, the polymeric fraction obtained from the HPLC separation was analyzed solely by means of HR-ESIMS, since the quantities of the isolated compounds did not allow a reliable NMR-based investigation. The mass spectrum revealed a quite complex composition showing a number of mono- and doubly charged ion peaks centered at *m/z* 765.2152 ($[C_{73}H_{78}O_{36}]^{2+}$; $\Delta = 2.665$ ppm), 1042.2858 ($[C_{98}H_{108}O_{50}]^{2+}$; $\Delta = -8.710$ ppm), 1046.3032 ($[C_{100}H_{108}O_{49}]^{2+}$; $\Delta = 5.533$ ppm), 1055.2985 ($[C_{100}H_{110}O_{50}]^{2+}$; $\Delta = -3.974$ ppm), and 1073.3092 ($[C_{50}H_{57}O_{26}]^+$; $\Delta = -3.799$ ppm).

According to previous reports [15], the doubly charged ion peaks at 765 and 1042 were attributed to an ethylene-linked Mv3gl trimeric and tetrameric compound, respectively; the peak at 1073 was assigned to an analogue of **4** mono-substituted with a vinyl group at either position 8 or 6 [16]. The two doubly charged ion peaks at 1046 and 1055 were tentatively assigned to an unreported ethylene-linked Mv3gl tetramer under different forms as depicted in SI.3. Further studies are being carried out with the purpose of isolating higher quantities of these compounds to confirm our structural hypotheses by NMR analysis. The

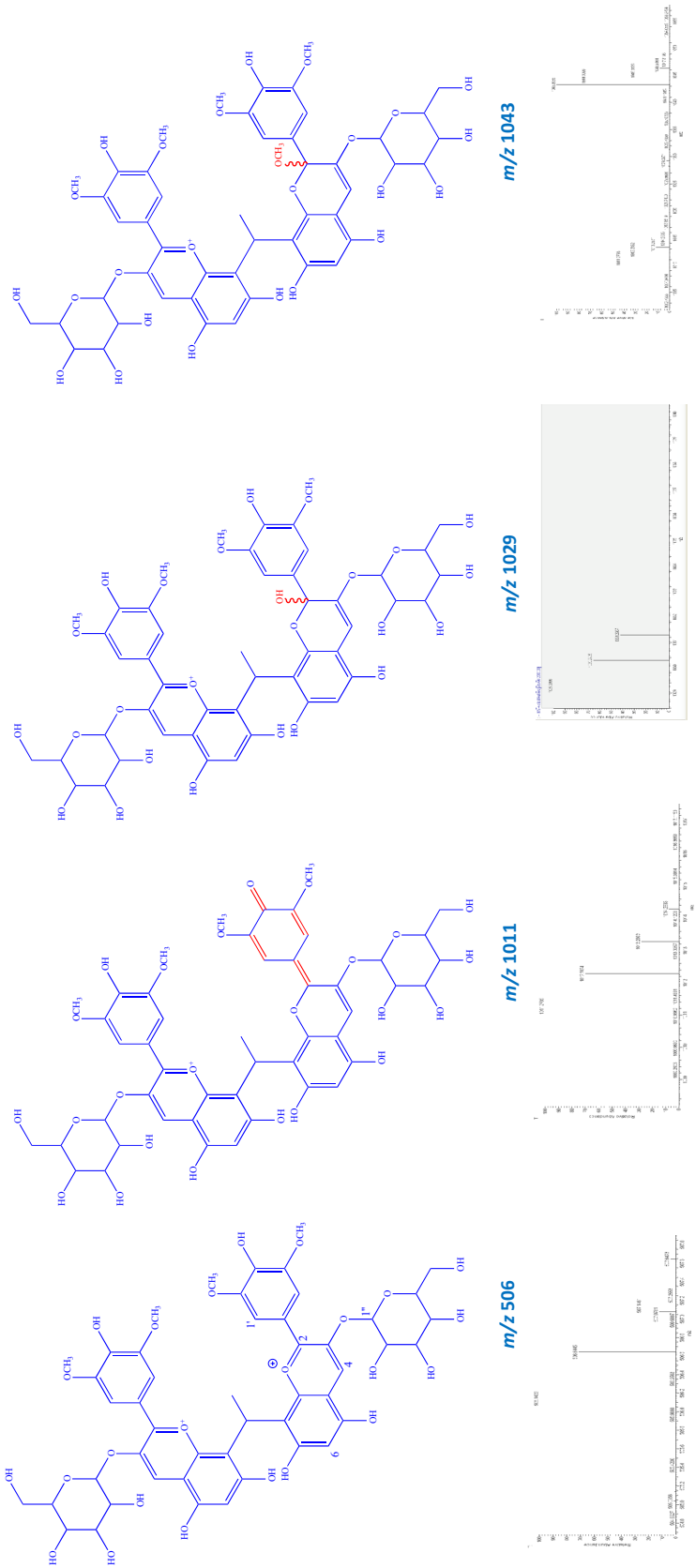

Fig. 3 Chemical structures of different forms of compound **4** (top) and associated MS spectra (below)

detection of the above polymers confirms that the anthocyanin C6 position is quite reactive towards electrophiles even if at a lesser extent than the C8 position.

Quite surprisingly, our NMR- and MS-based investigations conducted on the reaction solution A did not detect vitisin-B even at trace amounts.

A preliminary HPLC- and NMR-based analyses of the reaction solution B highlighted the presence of monomeric Mv3gl and the ethylene-linked Mv3gl dimer (**4**), along with other compounds (Fig. 4). To identify such compounds, a HR-ESIMS analysis was conducted. The MS spectrum contained, in addition to all the ion peaks detected in solution A, an abundant ion peak at *m*/*z* 809.2294 ($[C_{40}H_{41}O_{18}]^+$; $\Delta = 0.815$ ppm). This suggested the formation of ethylene-linked anthocyanin–flavanol condensation products [10]. Our hypothesis was consistent with the detected NMR resonances. According to data available in the literature [10], the presence of diasteroisomeric dimers constituted by Mv3gl and catechin linked by an ethylene moiety bridging the 8-positions of either subunit (**5**, **6**; SI.2; Fig. 4) was ascertained. The methine included in the ethylene bridge connecting the catechin and the anthocyanin subunits is an asymmetric carbon and this explains the existence of two diastereoisomers generating two parallel proton spin systems in the ^{1}H-NMR spectrum. By analogy with compounds **5** and **6,** the remaining resonances were assigned to another pair of diasteroisomers (SI.2; compounds **7** and **8)** constituted by a Mv3gl subunit and a catechin one bridged by an ethylene moiety linked to the catechin position 6 and the anthocyanin position 8 (Fig. 4). The occurrence of ethylene bridges between position 8 of Mv3gl and either position 8 or 6 of catechin was suggested by the conspicuously reduced intensities of NMR signals relative to both catechin H6 and H8 when compared to the other resonances, together with the lack of a resonance attributable to the Mv3gl H8 (Fig. 4).

The HPLC–DAD analysis was also useful to gain quantitative information on the formed products. Solutions A and B were analyzed after 2 h and 1 week of storage at 20 °C. Table 1 reports the concentrations of Mv3gl and of the identified pigments (**4**, **5**–**8**). The first surprising result was that the pigments were detected in the solutions already after 2 h and their amounts increased over time. On the basis of our results, we could conclude that acetaldehyde determined, almost immediately, the formation of the ethyl-linked dimer (**4**). In the presence of catechin, the formations of compounds **5–8** was favored over **4**, likely as a consequence of the better nucleophilicity of both C8 and, even though to a lesser extent, C6 of catechin when compared to the same positions of Mv3gl. Interestingly, in solution A, the amount of **4** slightly increased after 1 week, while the significant loss of Mv3gl could not be explained only by the formation of the dimer. Reasonably, this was due to degradation reactions leading to colorless products detected by HPLC–DAD at 280 nm (data not shown).

To investigate how and to what extent the formation of the identified pigments affected the color parameters, after 1 week of storage at 20 °C the reaction solutions A and B were subjected to chromatic and UV–Vis analyses (Table 2). It is reported that bathochromic and hyperchromic shifts as well as changes in terms of ΔE and Δhue are associated with co-pigmentation involving anthocyanins and catechins [11, 17–19].The shift to longer wavelengths (bathochromic shift) detected by us and shown in Table 2 is consistent with that observed by Lambert et al. [19], when a molar ratio 1:1 Mv3gl: catechin was used and when seed and skin extracts were added to an anthocyanin extract. Additionally, a significant hyperchromic effect of 36.7% by adding catechin was detected consistently with comparable positive effect noted by Lambert et al. [19]. Hence, in our study, the shift towards higher hue angle after adding catechin to the mixture of Mv3gl and acetaldehyde demonstrated that the bathochromic shift ascribed to co-pigmentation and to pigment formation was dominant.

A parameter useful to establish whether the observed changes in the chromatic properties are visually relevant is the colorimetric difference, ΔE, which summarizes all the chromatic variations between solutions containing only Mv3gl and acetaldehyde and those containing also catechin (Table 2). As a non-trained human eye is able to distinguish two colors with a ΔE value of 3.0 units CIELab [20], the results shown in Table 2 reveal perceptible color differences induced by the presence of catechin in the anthocyanin solution containing acetaldehyde.

Analysis of the reaction solutions containing Mv3gl, pyruvic acid (Solutions C) and catechin (Solution D); and of the reaction solutions containing Mv3gl, *p*-coumaric acid (Solutions E) and catechin (Solution F)

After 1 week of storage, the ^{1}H-NMR spectrum of both reaction solutions C and D contained only signals attributable to the unreacted starting reagents. Likewise, on account of their ^{1}H-NMR spectra in the solutions E and F, no major reactions apparently took place. The HPLC–DAD and colorimetric quantitative analyses of solution C showed that after 1 week, a slight loss of Mv3gl occurred (Table 1). Always after 1 week, in the presence of catechin (solution D), a more significant loss of Mv3gl was observed, probably due to two concomitant phenomena: (1) oxidation likely triggered by catechin; and (2) the formation of colorless high molecular weight compounds inferred by the occurrence of large chromatographic peaks at 280 nm (data not shown). The same behavior was observed for solutions containing

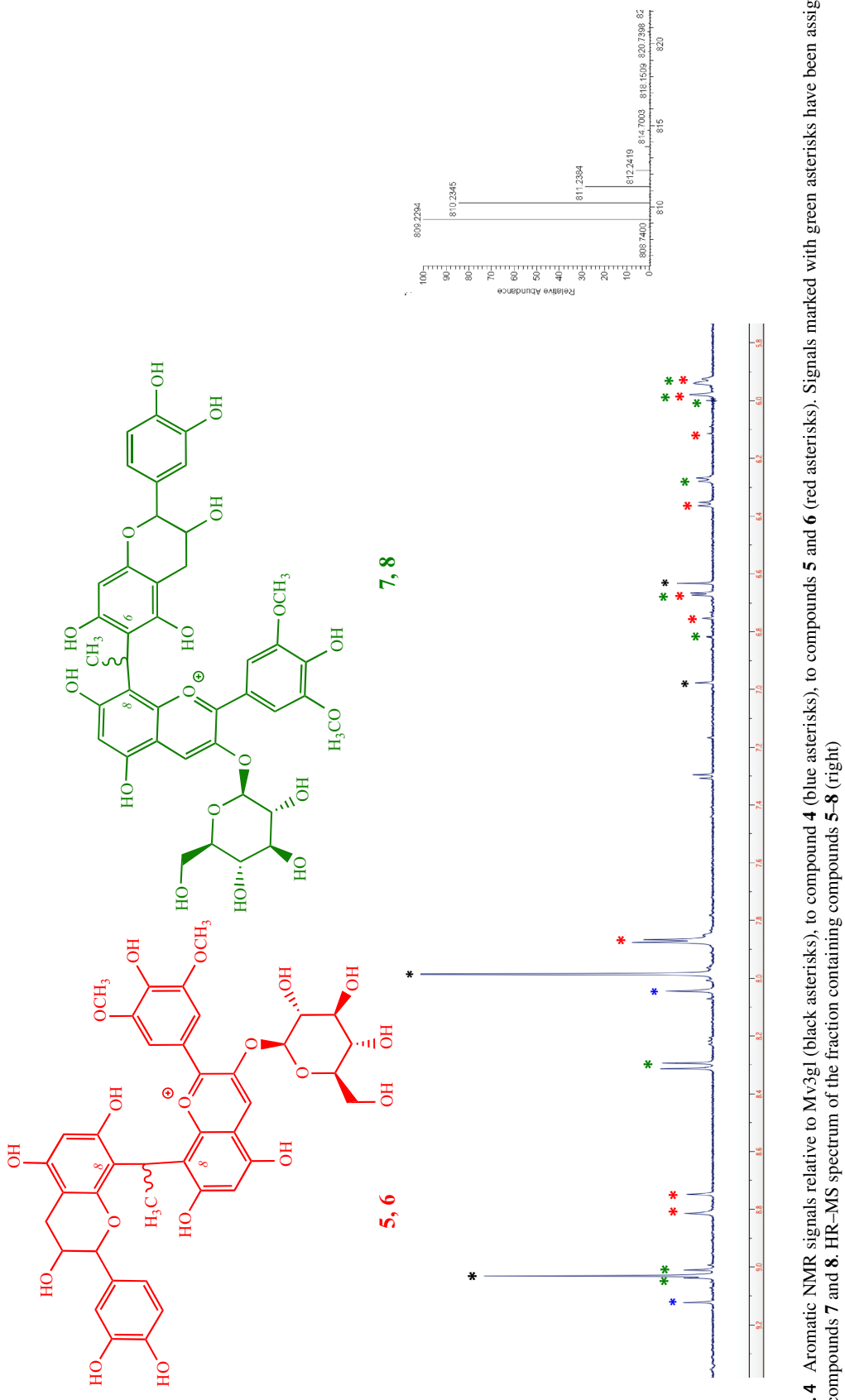

Fig. 4 Aromatic NMR signals relative to Mv3gl (black asterisks), to compound **4** (blue asterisks), to compounds **5** and **6** (red asterisks). Signals marked with green asterisks have been assigned to compounds **7** and **8**. HR–MS spectrum of the fraction containing compounds **5–8** (right)

Table 1 Concentration (mg/L) of Mv3gl and pigments detected in solutions A (Mv3gl + CH_3CHO), B (Mv3gl + CH_3CHO + Catechin), C (Mv3gl + pyruvic acid), D (Mv3gl + pyruvic acid + catechin), E (Mv3gl + *p*-coumaric acid), and F (Mv3gl + *p*-coumaric acid + catechin) by HPLC–DAD

Compound	Solution A		Solution B		Solution C		Solution D		Solution E		Solution F	
	2 h	1 week	2 h	1 week	2 h	1 week	2 h	1 week	2 h	1 week	2 h	1 week
Mv3gl	257 ± 41.9	161.2 ± 8.5	133.2 ± 40.4	77.0 ± 6.0	304.7 ± 20.1	232.0 ± 13.3	281.6 ± 24.9	159.8 ± 6.2	272.2 ± 9.1	103.1 ± 27.5	280.1 ± 9.3	159.3 ± 0.8
4	19.3 ± 1.8	20.5 ± 0.8										
5, 6	–		5.6 ± 0.7	7.3 ± 0.1								
			11.9 ± 2.8	15.6 ± 1.2								
7, 8	–		10.2 ± 2.3	13.1 ± 1.0								

p-coumaric acid. A remarkable difference was that already after 2 h of storage the loss of Mv3gl due to concomitant formation of colorless compound in presence of *p*-coumaric acid was higher than in solution C. Both pyruvic and *p*-coumaric acids appeared to be not as effective as acetaldehyde in enhancing wine color by forming red pigments. This is likely due to the concomitant production of anthocyanin colorless degradation products.

As already observed when catechin was added to solution A, a decrease of L^*, a higher chromaticity and hue angle was registered even when pyruvic acid was used (Table 2). Instead, the addition of catechin to the solution containing *p*-coumaric acid determined a decrease of the chromaticity and of the hue angle (Table 2). In all cases, differences in terms of ΔE were under the perceptibility threshold of a non-trained human eye. Also, variations of hue and bathochromic shifts were not significant, while a noteworthy hypochromic effect was detected. This might be due to the fact that, when added to solutions containing Mv3gl along with either pyruvic acid or *p*-coumaric acid, catechin caused a disruption of co-pigmentation that, as opposed to solution B containing acetaldehyde, was not balanced by the formation of pigments. It is reasonable to conclude that co-pigmentation between flavanols and anthocyanins is characterized by a hypsochromic shift when compared to the absorbance of anthocyanin self-association.

Conclusions

Among the wine metabolites (i.e. acetaldehyde, pyruvic acid and *p*-coumaric acid) employed in combination with Mv3gl in our reaction solutions, only acetaldehyde turned out to be reactive towards the anthocyanin, as opposed to pyruvic and *p*-coumaric acids that did not undergo any significant reactions. We could conclude that the nucleophilicity of either acid appeared to be too weak to attack the anthocyanin electrophilic C4 to form pyranoanthocyanins. Acetaldehyde possesses both an electrophilic center (the carbonyl functionality) and a nucleophilic one at its alpha position. By acting as an electrophile, acetaldehyde mediates self-condensation of anthocyanins by producing ethylene-linked pigments, characterized by hypsochromic shifts towards violet hues. On the other hand, as a nucleophile, acetaldehyde is believed to attack the electrophile C4 of the flavylium ion, thus producing, after an oxidation step, vitisin-B [7]. However, our experiments clearly indicated that at low pH levels, when anthocyanins predominantly exist as flavylium species, thus featuring simultaneously electrophilic centers at C2 and C4 along with nucleophilic centers at C6 and C8, the preferential reaction in the presence of acetaldehyde is the nucleophilic addition by the Mv3gl C8 to the acetaldehyde carbonyl functionality. Indeed, vitisin-B was not detected

Table 2 Colorimetric measurements and colorimetric and visible spectra differences following the addition of catechin to solutions A and B containing Mv3gl and acetaldehyde, solutions C and D containing Mv3gl and pyruvic acid, and solutions E and F containing Mv3gl and *p*-coumaric acid

	L^*	$a(u)^*$	$b(v)^*$	Chromaticity	Hue Angle	ΔE	Δhue	λ–λ_0 (nm)	(A-A0)/A0 × 100%
Solution A	75.71 ± 0.04	50.37 ± 0.07	17.52 ± 0.07	53.33 ± 0.09	19.18 ± 0.04				
Solution B	74.17 ± 0.01	50.80 ± 0.02	18.86 ± 0.03	54.19 ± 0.03	20.36 ± 0.02				
Colorimetric differences between solutions A and B following the addition of catechin						10.8	1.18		
Visible spectra differences between solutions A and B following the addition of catechin								4	36.7
Solution C	76.86 ± 0.01	50.44 ± 0.00	16.90 ± 0.00	53.19 ± 0.00	18.53 ± 0.01				
Solution D	74.80 ± 0.02	51.05 ± 0.04	18.17 ± 0.05	54.19 ± 0.05	19.59 ± 0.01				
Colorimetric differences between solutions C and D following the addition of catechin						2.1	−1.18		
Visible spectra differences between solutions C and D following the addition of catechin								1.5	−12
Solution E	63.87 ± 0.02	49.90 ± 0.01	6.95 ± 0.02	50.38 ± 0.01	7.93 ± 0.02				
Solution F	55.94 ± 0.02	45.21 ± 0.01	1.27 ± 0.01	45.23 ± 0.01	1.60 ± 0.01				
Colorimetric differences between solutions E and F following the addition of catechin						1.76	−1.06		
Visible spectra differences between solutions E and F following the addition of catechin								2	−18.8

in our reaction solutions. This observation is somehow consistent with what reported by Oliveira et al. (2009) that succeeded in setting up a hemi-synthesis of vitisin-B with a 30% yield only using vinyloxy-trimethylsilane to enhance the nucleophilicity of acetaldehyde. This implies that further and in-depth studies are necessary to clarify the mechanism of formation of pyranoanthocyanins in wines as well as their real role in wine color persistence.

In conclusion, our study demonstrated that it is acetaldehyde to play a significant role in the formation and evolution of red wine color. In fact, in the presence of anthocyanins, acetaldehyde mediates the rapid formation of ethylene-linked pigments that significantly affects the color of red wine, while reasonably stabilizing it over time. In fact, such pigments at wine pH preferentially exist with a cationic moiety [15] thus maintaining their colorimetric properties as opposed to monomeric anthocyanins that, in addition to being subjected to degradation over time, at wine pH, are mostly occurring as colorless hemiacetal pseudobases.

These results propel further studies aimed at analyzing the physical–chemical properties of such pigments and, particularly, their preferential conformations. The investigation of the still unexplored conformational space of these pigments, by means of molecular modeling techniques, might help the understanding of the chemical reasons why pigments are much more resistant than monomeric anthocyanin to pH variations and bleaching.

Compliance with ethical standards

Conflict of interest The authors declare that they have no conflict of interest.

Ethical approval This article does not contain any studies with human or animal subjects.

References

1. Brouillard R, Dangle O (1994) Anthocyanins molecular interaction: the first step in the formation of new pigments during wine aging? Food Chem 51:365–371
2. Mateus N, Silva AMS, Santos-Buelga C, Rivas-Gonzalo JC, De Freitas V (2002) Identification of anthocyanin-flavanol pigments in red wines by NMR and mass spectrometry. J Agric Food Chem 2110–2116
3. Boulton R (2001) The copigmentation of anthocyanins and its role in the color of red wine: a critical review. Am J Enol Vitic 52:67–87

4. Brouillard R, Dubois JE (1977) Mechanism of the structural transformations of anthocyanins in acidic media. J Am Chem Soc 99:1359–1364
5. Mateus N, De Freitas V (2001) Evolution and stability of anthocyanin-derived pigments during Port wine aging. J Agric Food Chem 49:5217–5222
6. Fulcrand H, Benabdeljalil C, Rigaud J, Cheynier V, Moutounet M (1998) A new class of wine pigments generated by reaction between pyruvic acid and grape anthocyanins. Phytochemistry 47:1401–1407
7. Oliveira J, De Freitas V, Mateus N (2009) A novel synthetic pathway to vitisin B compounds. Tetrahedron Lett 50:3933–3935
8. Fulcrand H, Cameira dos Santos PJ, Sarni-Manchado P, Cheynier V, Bonvin JF (1996) Structure of new anthocyanin-derived wine pigments. J Chem Soc Perkin Trans 1:735–739
9. Bakker J, Timberlake CF (1997) Isolation, identification, and characterization of new color-stable anthocyanins occurring in some red wines. J Agric Food Chem 45:35–43
10. Lee DF, Swinny EE, Jones GP (2004) NMR identification of ethyl-linked anthocyanin–flavanol pigments formed in model wine ferments. Tetrahedron Lett 45:1671–1674
11. Gonzalez-Manzano S, Santos-Buelga C, Dueñas M, Rivas-Gonzalo JC, Escribano-Bailón T (2008) Colour implications of self-association processes of wine anthocyanins. Eur Food Res Technol 226:483–490
12. Dangles O, Fenger JA (2018) The chemical reactivity of anthocyanins and its consequences in food science and nutrition. Molecules 23:1970
13. Forino M, Gambuti A, Luciano P, Moio L (2019) Malvidin-3-*O*-glucoside chemical behavior in the wine pH range. J Agric Food Chem 67:1222–1229
14. Oliveira CM, Ferreira ACS, De Freitas V, Silva AMS (2011) Oxidation mechanisms occurring in wines. Food Res Int 44(5):1115–1126
15. Atanasova V, Fulcrand H, Le Guernevé C, Cheynier V, Moutounet M (2002) Structure of a new dimeric acetaldehyde malvidin-3-glucoside condensation product. Tetrahedron Lett 43:6151–6153
16. Fulcrand H, Duenas M, Salas E, Cheynier V (2006) Phenolic reactions during winemaking and aging. Am J Enol Vitic 57:289–297
17. Mirabel M, Saucier C, Guerra C, Glories Y (1999) Copigmentation in model wine solutions: occurrence and relation to wine aging. Am J Enol Vitic 50(2):211–218
18. Berké B, De Freitas V (2007) A colorimetric study of oenin copigmented by procyanidins. J Sci Food Agric 87(2):260–265
19. Lambert SG, Asenstorfer RE, Williamson NM, Iland PG, Jones GP (2011) Copigmentation between malvidin-3-glucoside and some wine constituents and its importance to colour expression in red wine. Food Chem 125:106–115
20. Martinez JA, Melgosa M, Pérez MM, Hita E, Negueruela AI (2001) Visual and instrumental color evaluation in red wines. Food Sci Technol Int 7(5): 439–444